International Conference on Space Optics—ICSO 2018

Chania, Greece

9–12 October 2018

Edited by Zoran Sodnik, Nikos Karafolas, and Bruno Cugny

On-sky performance verification of near infrared eAPD technology for wavefront sensing at ground based telescopes, demonstration of e-APD pixel performance to improve the sensitivity of large science focal planes and possibility to use this technology in

G. Finger

Ian Baker

D. Alvarez

F. Eisenhauer

et al.

International Conference on Space Optics — ICSO 2018, edited by Zoran Sodnik, Nikos Karafolas, Bruno Cugny, Proc. of SPIE Vol. 11180, 111806L · © 2018 ESA and CNES · CCC code: 0277-786X/18/$18 · doi: 10.1117/12.2536156

On-sky performance verification of near infrared eAPD technology for wavefront sensing at ground-based telescopes, demonstration of e-APD pixel performance to improve the sensitivity of large science focal planes and possibility to use this technology in space.

G. Finger[*a], I. Baker[b], D. Alvarez[a], F. Eisenhauer[c], G. Hechenblaikner[a] D. Ives[a], L. Mehrgan[a], M. Meyer[a], J. Stegmeier[a], H. J. Weller[b]
[a]European Southern Observatory, Karl Schwarzschildstrasse 2, D-85748-Garching, Germany; [b]Leonardo, Southampton, Hants, SO15 OLG, UK; [c]Max Planck Institute for Extraterrestrial Physics, Garching, Germany

ABSTRACT

Ground based near infrared adaptive optics as well as fringe tracking for coherent beam combination in optical interferometry required the development of high-speed sensors. Because of the high speed, a large analog bandwidth is needed. The short exposure times result in small signal levels which require noiseless detection. Both of these conflicting requirements cannot be met by state-of-the-art conventional CMOS technology of near infrared arrays as has been attempted previously[1][2]. The HgCdTe electron avalanche photo diode (eAPD) technology is the only way to overcome the limiting CMOS noise barrier of near infrared sensors. Therefore, ESO funded the development of the near infrared SAPHIRA 320x256 pixel e-APD arrays at LEONARDO [3][4][5][6][7]. SAPHIRA arrays have now become the devices of choice for control loops with unsurpassed performance [21]. This has also been demonstrated by the four wavefront sensors and the fringe tracker deployed in the VLTI instrument GRAVITY which set a new sensitivity standard in infrared interferometry [8][9]. It has also been demonstrated that APD arrays have extremely low dark current (1E-3 electrons/s/pixel) and may outperform conventional CMOS arrays for 100 second integrations when operated with moderate APD gains. For AO systems of extremely large telescopes and for co-phasing segmented mirror telescopes larger formats are needed. Therefore, a 512x512 pixel SAPHIRA array with 64 parallel video outputs optimized for pyramid wavefront sensing is in development. Since the SAPHIRA array has successfully passed radiation hardness testing it soon may be used for future instruments in space. Apart from the large array common voltage for high APD gain it can also be operated with voltages compatible with the space qualified SIDECAR ASIC [10].

Keywords: avalanche photodiode, eAPD, HgCdTe, readout noise, excess noise, APD gain, cryogenic amplifier, near infrared, wavefront sensor, fringe tracker, LmAPD

1. INTRODUCTION

For high-speed near infrared sensors a major improvement of sensitivity can only be achieved by amplifying the photoelectron signal directly at the point of absorption by means of avalanche gain inside the infrared pixel. HgCdTe is the ideal detector material for near infrared eAPDs since the mass of the electron is much smaller than the mass of the holes and the APD process results in pure electron multiplication. Furthermore, unlike silicon HgCdTe is a direct semiconductor and phonons are not needed to generate an electron-hole pair. Hence, HgCdTe offers noiseless avalanche gain and excess noise factors close to unity have been measured [6]. For low dark current and high APD gain heterojunctions deliver the optimum performance with a wide bandgap absorber layer (λ_c=2.5 µm) for low dark current and a narrow bandgap gain region (λ_c=3.5 µm) for high APD gain.

*gfinger@eso.org, phone +498932006256; fax +49-89-32006530 ; www.eso.org/~gfinger

2. ROIC

The fringe tracker of GRAVITY needs to read out 48 dispersed fringes each 5 pixels wide and the wavefront sensor of GRAVITY needs to read out a window of 72x72 pixels. It was obvious that a new ROIC design was necessary to meet the windowed readout requirements of GRAVITY in an optimum way. To limit the analog bandwidth for high frame rates the array has 32 parallel outputs. To increase the frame rates of subarrays the 32 outputs of the ROIC are organized in such a way that they read out 32 adjacent pixels in a row at the same time. This ensures that all outputs are still used when reading subarrays in contrast to the Teledyne Hawaii-xRG arrays, in which each output reads a contiguous stripe of the detector and where for small subarrays only a single output can be used. However, with the SAPHIRA readout topology shown in Figure 1 the window size must be a multiple of 32 in the row direction, whereas there are no size restrictions in the column direction. The regions of interest and the regions which are reset can be separately downloaded in advance through a serial programming interface. The unit cell of the ROIC is a state-of-the-art low noise source follower. The array operates in the capacitive discharge mode, which allows multiple nondestructive readouts and Fowler sampling.

The time to read out a full frame is 512µs and it is scaling with the window size for smaller windows. Both the fringe tracker and the wavefront sensors of GRAVITY do not need to read the full frame. The 48 spectrally dispersed fringes of the fringe tracker can be read by 24 separate windows of 32x3 pixels. All spectra can be read in 14.4µs. The 68 active subpupils of the CIAO wavefront sensor, which are sampled by 8x8 pixels, require a window size of 96x72 pixels, which can be read in 48 µs. Therefore, at a closed loop bandwidth of 1 KHz the CIAO wavefront sensor can do Fowler sampling with 11 Fowler pairs to further reduce the readout noise.

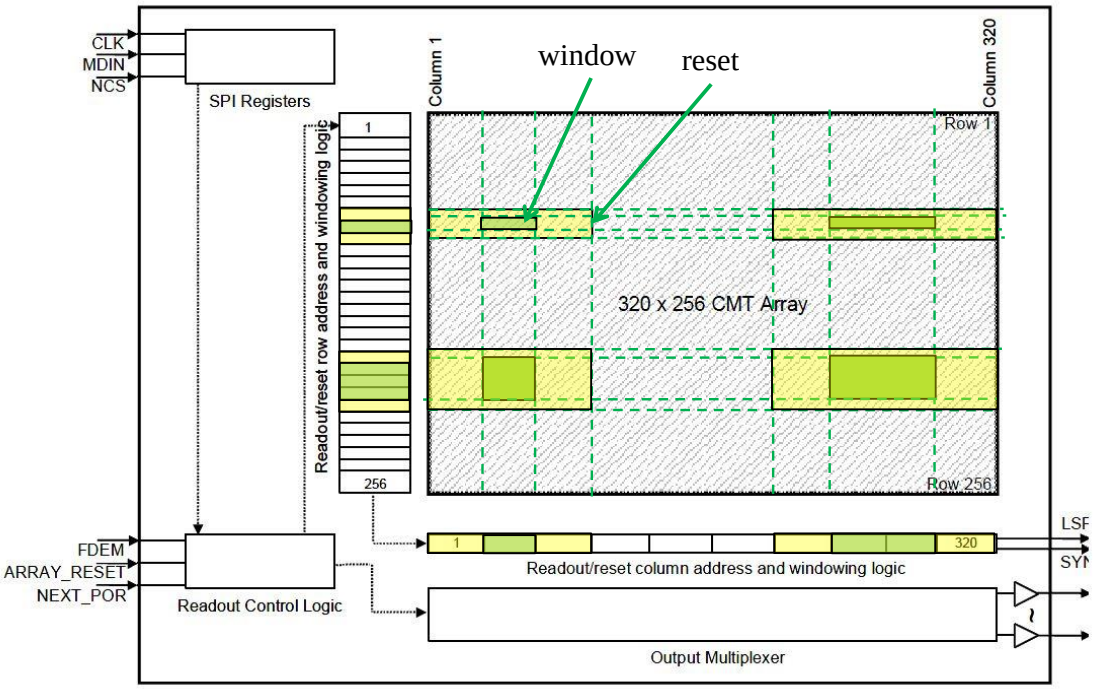

Figure 1 Layout of the SAPHIRA ROIC with predefined regions of interest (green) and reset regions (yellow). Regions of inter-est and reset regions can be predefined allowing different integration times in different windows.

3. DIODE STRUCTURE

The first eAPD arrays were grown with liquid phase epitaxy (LPE). Soon it became clear that the options of solid state engineering are very promising because they allow to tailor the diode bandgap and the doping of different layers to a specific application. These structures are heterojunctions and require the replacement of the LPE growth technology with metal organic vapour phase epitaxy (MOVPE). The first high performance λ_c=2.5 µm HgCdTe arrays hybridized to the SAPHIRA ROIC were Mark3 diode designs shown on the left side of Figure 2. Iterations of the HgCdTe manufacturing techniques and bandgap structures are denoted by the mark number. The arrays are mesa heterojunctions grown by MOVPE on a cheap GaAs substrate, which is then removed by a chemical etch. The top layer is a CdTe seed layer which is opaque at wavelengths λ<0.8 µm. A thick wide bandgap buffer layer is used to cope with the lattice mismatch of GaAs. This buffer layer limits the spectral response of Mark3 on the short wavelength side to wavelengths λ>1.3 µm. A mesa slot extending through the absorber layer electrically isolates the pixels. Photons are absorbed in the p-type absorber. The photon-generated charge diffuses to the p-n junction and is then accelerated in the electric field of the multiplication region to start the multiplication process by impact ionization. To boost the avalanche gain, the multiplication region is made of narrow bandgap material corresponding to a cutoff wavelength of λ_c=3.5 µm. The Mark3 diode arrays are currently deployed in the GRAVITY instrument at the VLTI [8].

To include the astronomically important Y and J bands in the spectral range of eAPDs, the Mark14 diode structure was developed at Leonardo. It was funded by the University of Hawaii [13][14]. To extend the spectral response down to λ=0.8 µm the wide bandgap buffer layer had to be removed as shown in Figure 2. The absorber layer is directly grown on CdTe by a pauseless process as shown in the middle of Figure 2. The p-type absorber is now much thicker and therefore requires much longer diffusion lengths for the photon-generated charge to reach the diode junction. This is achieved by a high temperature anneal. The right side of Figure 2 shows a photograph of the pixel mesa structures with the indium bumps on the top. The cone structure of the mesa acts as a light concentrator for the diode junction reducing the optical crosstalk, as shown by the drawing below the photograph on the right side of Figure 2.

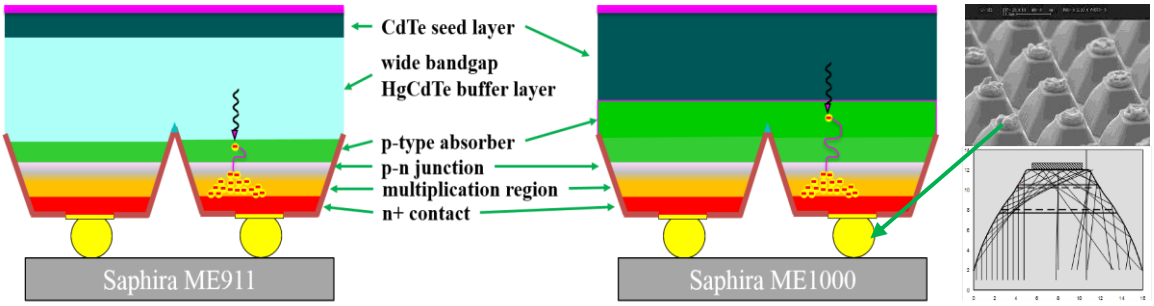

Figure 2 Left: Mark3 MOVPE diode design with wide bandgap buffer layer limiting s short wavelength response to λ>1.3 µm. Right: Mark14 MOVPE diode design without wide bandgap buffer layer sensitive from 0.8 to 2.5 µm

4. TEST RIG

The SAPHIRA array has 32 parallel video channels. In our setup the video outputs are amplified directly at the cold focal plane on the detector board with off-chip cryogenic preamplifiers as shown in Figure 3. The cryogenic preamplifiers are commercial off the shelf linear CMOS operational amplifiers, the OPA 354, which has a gain-bandwidth product of 100MHz and a noise of only 6.5nV/√Hz. It provides the needed pixel rate of 5Mpixel/s/channel and operates reliably at cryogenic detector temperatures down to T=40K. The preamplifier design matches the differential input stage of the 10 MHz 32 channel ADC board with a VIRTEX-6 FPGA for fast preprocessing of Fowler samples and preprocessing of subpixel samples.

Figure 3 : Detector board with flex cable, two 72-pin Micro-D connectors for penetrating the radiation shield and the 128 pin HIREL vacuum connector.

For the evaluation of the performance of the eAPD array the detector is mounted in the IRATEC test camera shown in Figure 4. The camera optics consists of a cold f/11 Offner relay with a cold pupil and two cold filter wheels in front of the detector. One wheel is equipped with bandpass filters and the other wheel with neutral density filters. To cool down the camera a liquid nitrogen continuous flow precooling system is used. The detector can be cooled down to a temperature of 40 K by a two-stage closed cycle cooler. A warm test pattern with a grid of holes in front of the camera entrance window is illuminated by an extended blackbody and imaged onto the detector by the Offner relay. By changing the temperature of the blackbody, a test pattern of calibrated intensity can be generated and imaged onto the detector. In the movie shown at [11] a chopper at ambient temperature was put between this test pattern and the blackbody. The test pattern was observed in filter H and the blackbody temperature was set such, that the flux level at the holes varies for the two copper phases between 0.38 photons/DIT/pixel and 1.29 photons/DIT/pixel with DIT 1.17ms. The holes can be clearly seen. This allows a relative comparison of the performance of different detectors in terms of signal to noise without uncertainties due to issues of absolute efficiency calibrations.

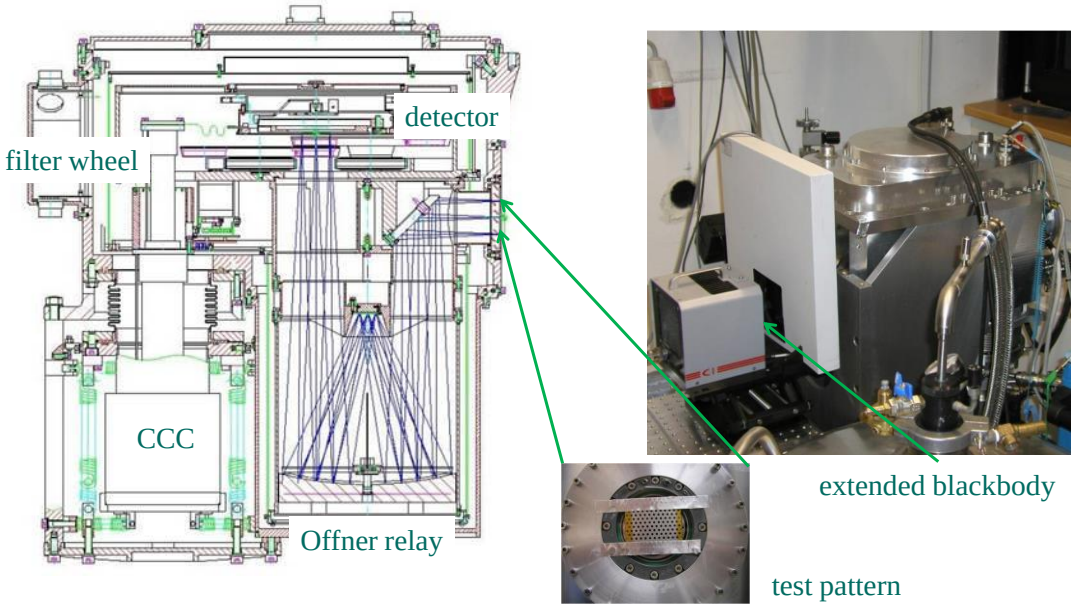

Figure 4 Test setup with IRATEC camera, cold optics and cold filter wheel. Test pattern with grid of holes illuminated by extended blackbody and imaged by f/11 Offner relay onto detector.

5. TEST RESULTS

At short integration times in the millisecond range the SAPHIRA array achieves subelectron noise and the APD gain is 700 at a bias voltage of 19V. The array at high APD gain still has superb cosmetic quality and achieves a readout noise

of less than 0.2 electrons rms with Fowler sampling at a frame rate of 1KHz, as has been shown in the previous ICSO conference [12] and at SPIE [6]. The measured excess noise factor is close to unity and the avalanche gain process is almost noiseless because HgCdTe is a direct semiconductor. For near infrared control loops the SAPHIRA eAPD arrays are mature devices with unmatched performance[21].

The Mark14 arrays are the first devices without the wide bandgap buffer layer [13][14]. Therefore, it was of great interest to measure the spectral quantum efficiency over the entire sensitive range from λ=0.8μm to λ=3.5 μm. For this purpose, a grating spectrometer was put on the optical bench in front of the test camera. The spectrometer was illuminated by a blackbody cavity which can be heated to a temperature of T=1200C. The exit slit of the monochromator is imaged by the cryogenic Offner relay onto the detector [6]. The efficiency of the monochromator is calibrated by mounting a pyroelectric detector on the exit slit of the monochromator. The wavelength dependence of the quantum efficiency obtained in this way is only a relative efficiency. It must be scaled to the absolute quantum efficiency measured in H and K band taking images of an extended blackbody in front of camera. The absolute quantum efficiency is indicated by horizontal bars in Figure 5. At shorter wavelengths the quantum efficiency drops. A major part of this drop (~15%) may be attributed to the antireflection coating which is optimized for a wavelength of λ=2.1 μm, as indicated by the violet dash-dotted curve in Figure 5. At unity APD gain, represented by the solid line in Figure 5, the array is sensitive from λ=0.8 μm to λ=3.5 μm. The quantum efficiency in Figure 5 is defined as the number of electrons per incident photon measured at the output pin of the detector divided by the APD gain. The quantum efficiency QE(λ) is high over the entire sensitive range from λ=0.8 μm to 2.5 μm.

The spectral quantum efficiency shows a modulation characteristic of interference fringes generated by multiple reflections in a parallel plate. If the wavelength scale is changed to wavenumbers the distance between maxima of the QE is equidistant and has an average value of 437/cm. This corresponds to a thickness of the CdTe seed layer of 4.24μm assuming a refractive index of n=2.7. This measured thickness of the CdTe agrees with the diode design.

For photons with a wavelength longer than the cutoff wavelength of the absorber layer, which is λc=2.5 μm, the absorber layer is transparent. The photons are absorbed in the multiplication layer, which has a cutoff wavelength of λc=3.5 μm. Since the quantum efficiency in Figure 5 is defined as the number of electrons per incident photon divided by the APD gain, for high APD the gain drops at wavelengths longer than the cutoff wavelength of the absorber layer, which is λc=2.5 μm. For an APD gain of 421 the quantum efficiency in Figure 5 is represented by the dash dotted curve. The full APD gain is only experienced by those electrons which have been generated by photons with wavelengths shorter than the cutoff wavelength of the absorber layer. Photons with longer wavelengths are absorbed in the multiplication region and the photon-generated electrons experience only a partial APD gain depending on the depth at which the photon was absorbed.

To obtain low dark currents with the SAPHRA ROIC ME1000 the ESO array was shipped to LEONARDO to tape off and shield a glow center which had been located by Dani Atkinson [14][15]. To achieve the low dark currents plotted as a function of APD gain at different detector temperatures in Figure 6, the operating voltages of the SAPHIRA ROIC were reduced from the nominal values of 5 V to 2.5 V. To minimize the multiplexer glow the voltage VDDOP of the output FET was even further reduced to 1.8V and the supply voltages of the off-chip cryogenic preamplifiers were reduced to 2.6 V.

At higher temperatures the temperature dependence of the dark current is mainly determined by the narrow bandgap multiplication region. At high APD gain the dark current is dominated by temperature independent trap assisted tunneling. The green dotted curve shows the model prediction of trap assisted tunnel current. Current research looks for ways to reduce trap assisted tunneling at higher APD gain. It is remarkable that for low APD gain at a temperature of T=40K the dark current of the SAPHIRA array is in the 1E-3 e-/s/pixel regime, which is as low as the values measured for the best large format 2Kx2K HgCdTe arrays. These low dark currents were measured by single on-chip detector integration times of up to 4 days sampling the integration ramp non-destructively every 10 minutes to check the linearity of the integration ramp. The large number of nondestructive readouts also allows the elimination of cosmic rays by discarding discontinuities of the integration ramp. The spectacular dark current result raises expectations that APD technology will eventually also break the CMOS noise barrier of conventional large format infrared arrays offering also noiseless detection for the most sensitive long-time exposures. The goal for long exposures is to become also limited by the Poisson statistics of photons emitted by the faintest astronomical sources.

An attempt was made as shown in Figure 7 to compare the readout noise of the SAPHIRA eAPD array with the readout noise of a Hawaii-2RG array for integration times of 100s [7]. To make a fair comparison the ratio of the total time spent on reading out the arrays nondestructively must be equal to the ratio of the array formats (2048^2/(320x256)). For the SAPHIRA array 64 Fowler pairs and for the Hawaii-2RG 4 Fowler pairs were used. The outputs of the SAPHIRA array are read at 5Mpix/s/channel and the Hawaii-2RG at 100Kpix/s/channel. The readout noise obtained with the SAPHIRA array at an APD gain of 7.7 is 2.8 electrons rms whereas the readout noise obtained with the Hawaii-2RG array is 6.5 erms. It will need further evaluation to determine why it was not possible to obtain subelectron readout noise with higher APD gain for integration times of 100 seconds. If the APD gain can be increased by a factor of 3 without increasing the dark current it should be possible to obtain subelectron readout noise for integration times of 100 seconds. This could be accomplished by increasing the bandgap in the multiplication region of the diode.

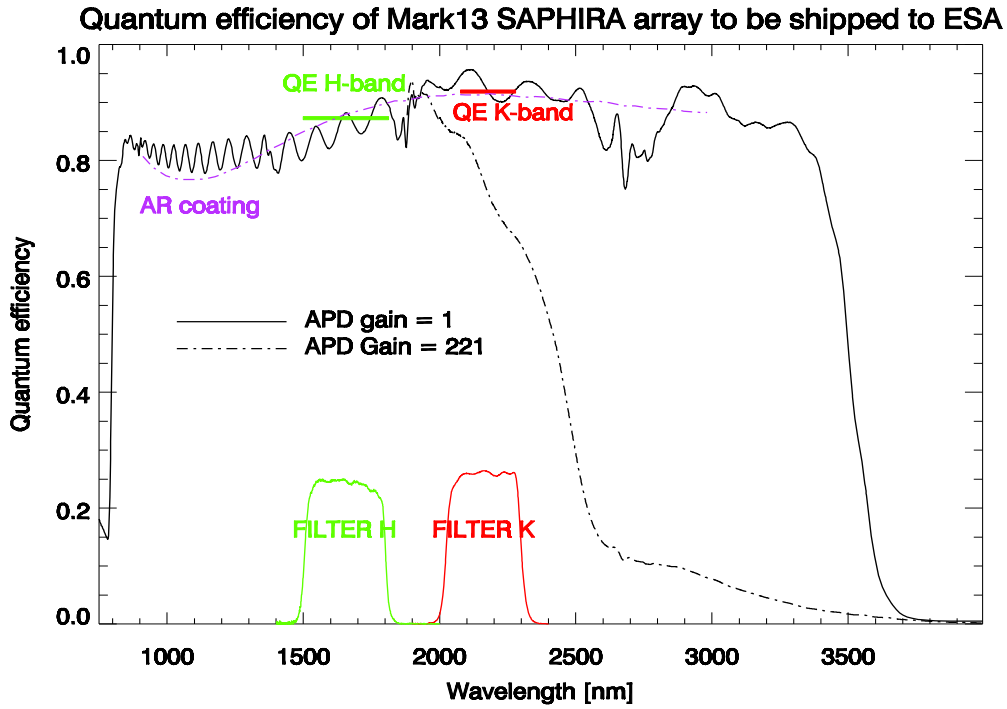

Figure 5 Quantum efficiency of Mark14 array versus wavelength for unity APD gain (solid curve) and APD gain of 421(dash-dotted curve). At unity APD gain cutoff wavelength is 3.5 μm due to narrow bandgap multiplication region. At high APD gain cutoff wavelength is 2.5 μm since photons with wavelengths longer than the cutoff wavelength of the absorber layer experience only partial APD gain. Absolute quantum efficiency is based on measurements with broad band H and K filters

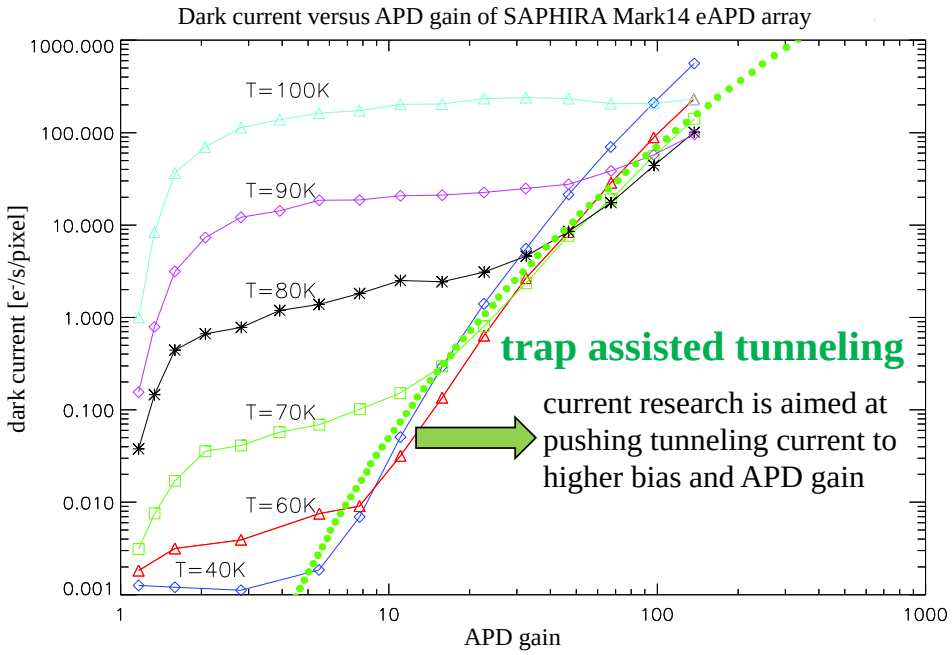

Figure 6 Dark current as a function of APD gain for different detector temperatures. At a detector temperature of T=40K and low APD gain dark current is 1E-3 electrons/s/pixel. At high APD gain dark current is dominated by temperature independent trap assisted tunneling. Current research is aimed at reducing trap assisted tunneling at higher APD gain.

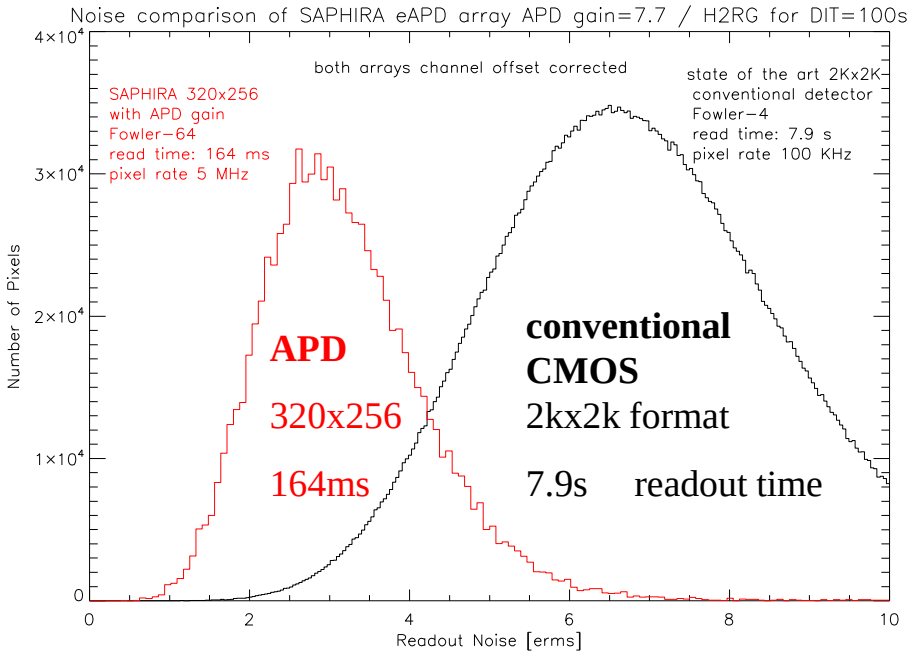

Figure 7 Comparison of the readout noise of SAPHIRA eAPD array with the readout noise of a Hawaii-2RG array. Integration time is 100s. For a fair comparison the ratio of the total time spent on reading out the arrays nondestructively is equal to the ratio of the number of pixels of the arrays (2048^2/(320x256)). For the SAPHIRA array with 64 Fowler pairs the readout noise is 2.8 erms and for the Hawaii-2RG array with 4 Fowler pairs the noise is 6.5 e-mrs. The outputs of the SAPHIRA array are read at a pixel rate of 5MHz and those of the Hawaii-2RG at 100KHz.

6. ON-SKY PERFORMANCE OF SAPHIRA IN GRAVITY

The Very Large Telescope VLT of the European Southern Observatory ESO was built with delay lines to coherently combine the light of the four 8-meter telescopes by the VLT interferometer VLTI . GRAVITY is a new VLTI instrument with fiber fed integrated beam combination of the four telescopes to do phase referenced imaging and narrow angle astrometry with an equivalent 130m diameter angular resolution and a collecting area of 200m^2 [8]. To correct the atmospheric piston, it has a fringe tracker for the dispersed fringes of the 6 beam combinations. The phase of each fringe is shifted optically four times by 90 degrees to determine the phase. With two polarizations 48 dispersed fringes must be read. The windowing function of the SAPHIRA ROIC was optimized for this application and the 48 spectra can be read in 14.4 µs and heavy Fowler sampling can be performed to achieve the required frame rate of 1KHz. Each of the four 8-meter telescopes is equipped with CIAO, the Coude Infrared Adaptive Optics system, which has a SAPHIRA near infrared Shack-Hartmann wavefront sensor needing a window of 96x72 pixels [16].

Both the fringe tracker and the wavefront sensors outperform the specifications of GRAVITY [8][16]. The Coude Infrared Adaptive Optics systems are located in the Coude rooms of the VLT telescopes and have bimorph deformable mirrors. The Shack-Hartmann wavefront sensors have 9x9 subapertures with a FOV of 4'' sampled by 8x8 pixels, as shown on the left side of Figure 8. The right side of Figure 8 shows the image of a star, taken with the PICNIC sensor in the tip tilt sensor of the VLTI Infrared Image Sensor IRIS during the CIAO commissioning, at the top with the AO loop open and at the bottom with the AO loop closed [16].

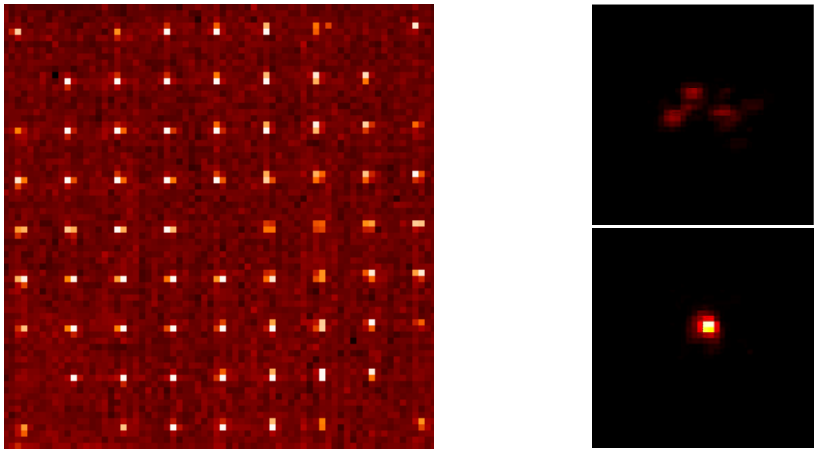

Figure 8 Left: Left: 9x9 subapertures of Shack-Hartmann sensor on 96x72 pixel window Right: at top image of star with AO loop open and at bottom with AO loop closed.

Figure 9 shows the closed loop rejection transfer function for Zernike modes up to order 44. Figure 10 shows the Strehl ratios as a function of seeing measured on a mK=6.5 magnitude star. For good seeing CIAO works on guide stars as faint as magnitude 11.

On the left side of Figure 11 fringes of IRS16C (mK=10) are shown which have been taken with the SAPHIRA fringe tracker to stabilize the dispersed science fringes (middle) of the star S2 (mK=14) in the Galactic center, shown as image on the right side. The previous VLTI instrument was PRIMA [17]. It used a PICNIC detector and could do fringe tracking up to a correlated magnitude of mK=8.5 with the 8-meter telescopes, while with GRAVITY the limiting magnitude for fringe tracking is about mK=11. The electron avalanche photodiodes improved the sensitivity for fringe tracking by more than 2 magnitudes. The limiting magnitude for coherent exposures with GRAVITY is mK~17 – this sets a new sensitivity standard in infrared interferometry, made possible by the deployment of eAPD technology, which is now widely being used in near infrared interferometry and for wavefront sensing [9][21].

The pericenter approach of star S2 to the massive black hole in the Galactic center has been observed in May 2018 and for the first time the gravitational redshift in the orbit of S2 has been detected and the relativistic Schwarzschild precession of the S2 orbit is being measured [9]. This is a spectacular on sky demonstration of the performance gain made possible with eAPD technology.

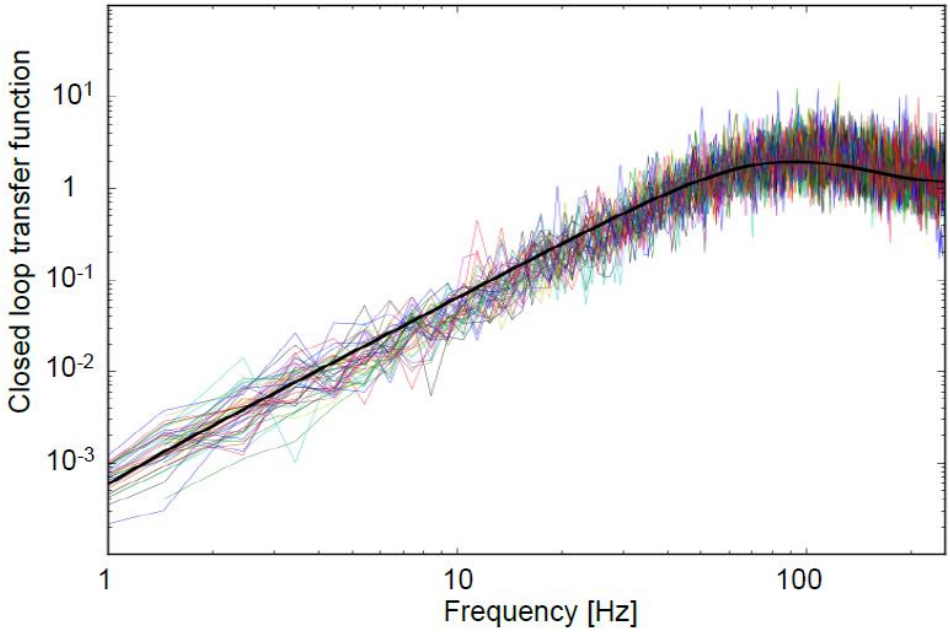

Figure 9 Coude Infrared Adaptive Optics (CIAO) closed loop rejection transfer function for Zernike modes up to order 44.

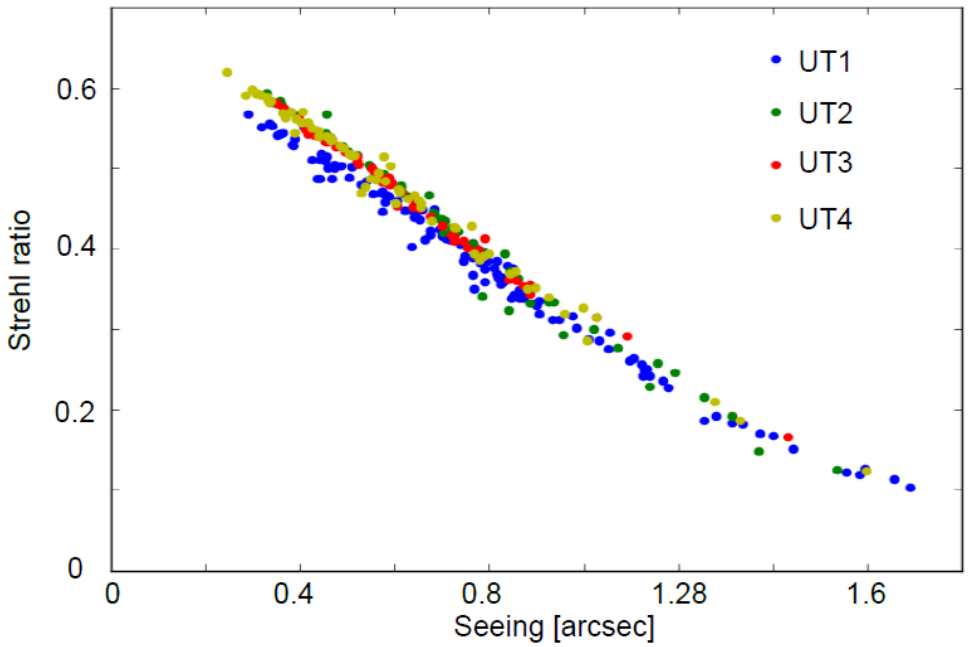

Figure 10 Strehl ratio of CIAO as a function of seeing for a star of magnitude 6.5.

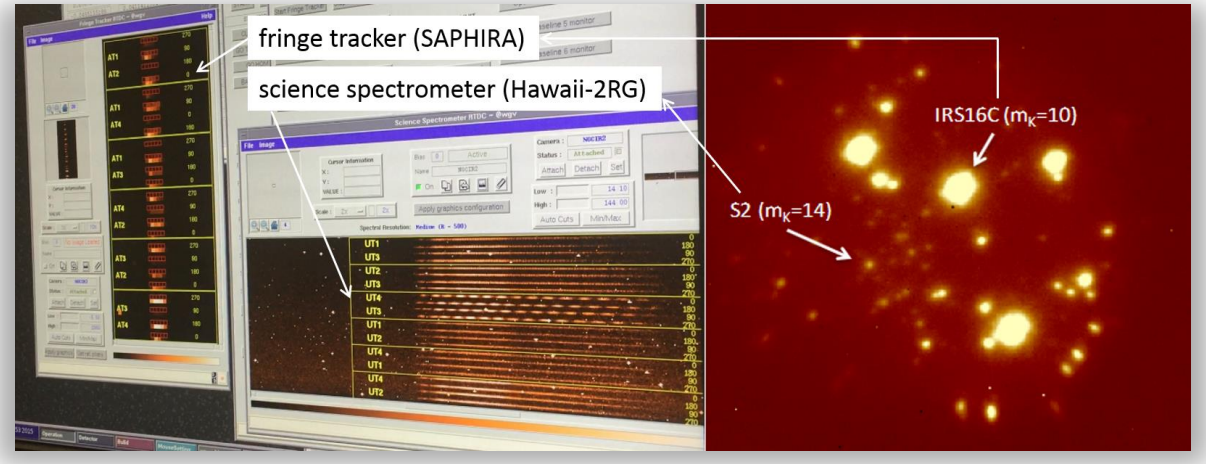

Figure 11 Dispersed and stabilized fringes of star S2 (mK =14) measured with science spectrometer. Right: Image of galactic center with S2 and IRS16C (mK =14), which is used for fringe tracking. Left: Dispersed spectra of IRS16C on SAPHIRA fringe tracker.

7. POTENTIAL USE OF EAPD TECHNOLOGY FOR SPACE

To qualify the 320x256 pixel eAPD SAPHIRA arrays for space applications tests of radiation hardness have been carried out. Two Mark 14 arrays were irradiated with a dose of 60 krad gamma radiation without any degradation of array performance. The array was also exposed to 50MeV proton radiation with a dose of 1E11/cm^2. Due to problems with the proton source the array was cold and powered but could not be not actively monitored during exposure and the transient response was not measured. It should be investigated if the proton causes a problem for the next exposure. However, the integration ramps taken in the lab with multiple nondestructive sampling show, that discontinuities in the integration ramp caused by cosmic events leave the integration ramp undisturbed after the event [7]. It looks like APDs are robust which is somewhat surprising but maybe due to weak lattice self-repairs. No variation in the avalanche process and no long-term degradation of the dark current has been observed so far. LEONARDO has permission from ESA to get the irradiated arrays tested for low dark current at ESO or at the University of Hawaii.

To achieve the extremely low dark currents of 1E-3 electron/s/pixel measured with the 320x256 pixel SAPHIRA eAPD array the operating voltages of the SAPHIRA ROIC were reduced from the nominal values of 5 V to 2.5 V. To minimize the ROIC glow the supply voltage VDD was reduced to 3.3V and the voltage VDDOP of the output FET was even further reduced to 1.8V, clock voltages were set to 0V/2.5V and the supply voltages of the off chip cryogenic preamplifiers were reduced to 2.6 V. With these voltage settings the operation of the SAPHIRA eAPD array becomes compatible with the SIDECAR ASIC which has been selected by NASA to become the FPA drive electronics for all shortwave infrared instruments on JWST [19][20]. There is only one voltage, the array common voltage which cannot be provided by the SIDECAR ASIC. Depending on the required APD gain it needs to be a large negative voltage of up to -15V. It has to be provided by a separate power supply. The SIDECAR ASIC has 36 fully differential 16 bit ADCs operating at 500KHz sample rate and 12 bit ADCs operating at 10 MHz. ESO has already operated the Hawaii-2RG array with 32 parallel 10 MHz ADCs [18]. Discussions are ongoing to set up a program to demonstrate the operation of the 320x256 pixel SAPHIRA array with the SIDECAR ASIC.

8. LARGE 512X512 PIXEL SAPHIRA ARRAY

The Mark3 eAPD array meets the requirements of the GRAVITY instrument in an optimum way. However, for the Extremely Large Telescope ELT the format of the current SAPHIRA 320x256 pixel array is too small. There are four ELT projects requiring a larger format of 512x512 pixels. All four ELT projects clearly prefer the current pixel size of 24µm instead of smaller pixel sizes of 15 µm pixel pitch, which has been selected for the large format low flux 1Kx1K science arrays operated in photon counting mode [22]. The larger pixel size facilitates optical alignment, mechanical tolerancing and stability. It also simplifies the lenslet arrays. The ELT projects needing the larger eAPD array are the wavefront sensor for the ELT pre-focal station, the sensor for co-phasing the ELT mirror segments, a pyramid wavefront sensor for the second-generation ELT Planetary Camera and Spectrograph PCS and a wavefront sensor for the mid-infrared imager and spectrometer METIS.

Apart from the detector for the PCS pyramid wavefront sensor, detector sensitivity is only required for the H and K band. The fringe sensor for the co-phasing of the ELT mirror segments does not need subelectron sensitivity but it requires speed and a large storage capacity at unity APD gain (3E5 electrons). The pyramid WFS for the planetary camera must be read out at a frame rate of 2KHz with double correlated sampling. But this frame rate is not required for the full frame. Only four windows of 150x150 pixels need to be read which can be located symmetrically to the center row of the array.

The 1Kx1K SAPHIRA development funded by the University of Hawaii is targeting at low dark current and large format in a low background environment to equip large format science focal planes [22]. Therefore, a separate low risk design of a 512x512 SAPHIRA array, which is optimized for high APD gain to achieve low noise at high speed is considered as the best and most cost-effective complementary solution for the ELT AO wavefront sensors.

The frame rate of 1 KHz for the full 512x512 pixel frame with double correlated sampling or 2 KHz with uncorrelated sampling can only be accomplished by either increasing the bandwidth of the video outputs or by increasing the number of parallel outputs. Increasing the bandwidth by more than a factor of 2 may be difficult for a 0.6 µm CMOS fabrication process. Increasing the number of outputs is a more conservative approach. As for the current 320x256 SAPHIRA array adjacent pixels shall be read out with a single conversion strobe. This readout topology will maintain the multiplex advantage for the readout of subarrays.

For all ELT projects it is acceptable to place windows symmetrically to the center row of the array. To keep line tracks short and to reduce capacitive loads the 512x512 pixel array could be divided into four quadrants, each of which is read out by 16 parallel video channels. In this case with a single conversion strobe all corresponding pixels of the four pupil images of a pyramid wavefront sensor can be read out simultaneously and the calculation of the wavefront errors can be started immediately with zero latency
.
If the array is only divided into an upper and a lower half each having 32 parallel video outputs the calculation of the wavefront can be only be started depending on the window size at latest after the readout of a complete row is finished. This introduces a maximum latency for the start of the calculation of 3.9 µs. This additional latency of 3.9 µs is negligible in terms of performance loss of the pyramid wavefront sensor. Considering the additional ROIC complexity of a four-quadrant solution and the negligible gain of AO performance it was decided to implement a solution with an upper and a lower half of the array which is more robust and simpler to implement.

Only the vertical readout direction needs to be programmable. Experience has shown that there is a substantial dc offset for the first few rows of a full frame read out. By starting the readout from the top and the bottom edge, this offset is not in the center of the array but at the top and bottom edges of the array where it is less disturbing. For pyramid wavefront sensing the vertical readout direction will be from top to bottom for both the upper and lower half of the array. In this way four subwindows can be read out concurrently in the upper and lower half of the array and calculation of the wavefront errors can already be processed during readout with minimum latency. Therefore, the vertical readout directions of the upper and lower half are programmable to either optimize the array for pyramid wavefront sensing (green arrows in Figure 12) or for minimizing discontinuities at the central rows (black arrows). The detector shall support a readout scheme as depicted in Figure 12.

With 64 parallel outputs the 2 KHz frame rate for an uncorrelated readout needs an analog bandwidth adequate for a pixel rate of 8.7 MHz per output. The current 320x256 pixel SAPHIRA array is read out with a pixel rate of 5MHz with no measurable cross talk due to bandwidth limitations. The ESO NGC controller has a 32 channel 10 MHz ADC board. Due to FPGA limitations of the ADC board the pixel rate is currently limited to 5 MHz. However, optimization of the VHDL code should achieve a pixel rate of 8.7MHz. With this optimization, the large SAPHIRA array can be operated at a frame rate of 2KHz with one frontend basic board and two 32-channel 10 MHz ADC boards. No further hardware development of the ESO NGC controller is needed to operate the large 512x512 SAPHIRA array at full speed.

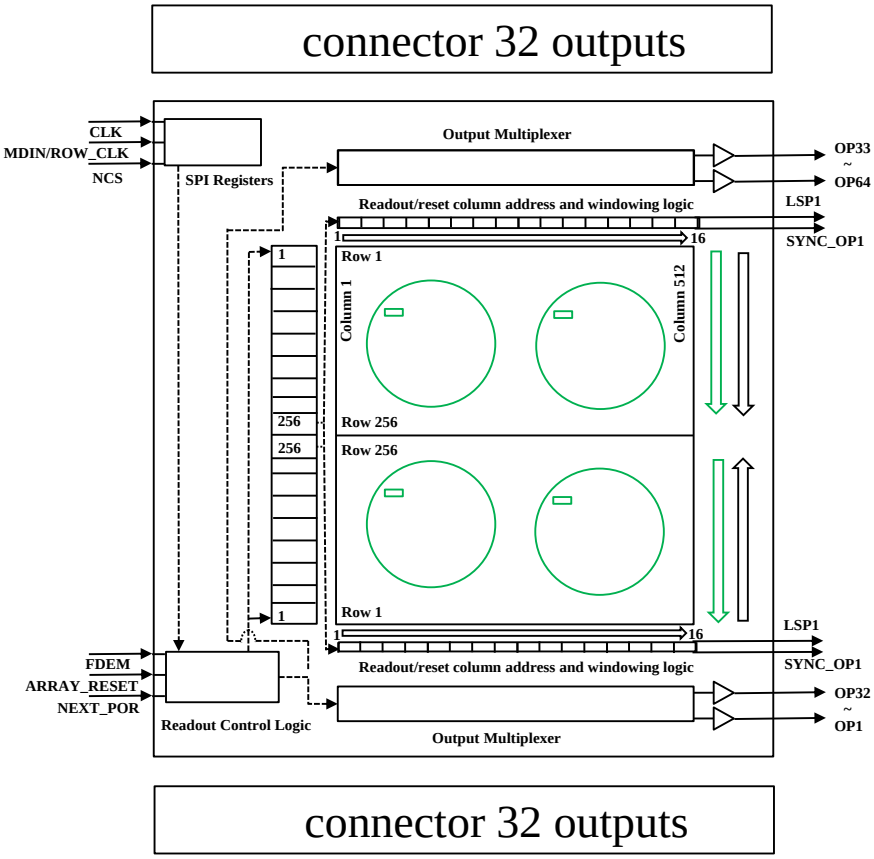

Figure 12: Proposed layout of the 512x512 pixel ROIC dividing the array into an upper and a lower half each having 32 parallel video outputs. Vertical and horizontal readout directions are programmable. Video outputs are at the top and the bottom of the array

9. CONCLUSION

For control loops in the near infrared as used in wavefront sensors of adaptive optics systems and in fringe trackers of interferometers the LEONARDO SAPHIRA eAPD arrays excel with subelectron readout noise at frame rates of 1KHz. These devices are mature and have become the devices of choice for these applications. With fife SAPHIRA arrays deployed in GRAVITY the gravitational redshift has been observed during the pericenter approach of star S2 to the massive black hole in the Galactic center. The pixel performance of the current SAPHIRA eAPD arrays and their extremely low dark current demonstrate that eAPD technology may also enable the next step in sensitivity for large science focal planes of future instruments on extremely large telescopes. They have the potential to offer subelectron readout noise for the long integration times required for detecting the faintest astronomical objects. The challenge will be to develop MOVPE diode structures keeping the dark current below 1.1 E-3 e^-/pixel/s with sufficient APD gain to achieve subelectron readout noise for integration times of 15 minutes. If an appropriate diode structure is developed

which can demonstrate a performance on sky which is superior to that of conventional infrared arrays, sufficient funding will be provided to develop large detector formats in buttable array packages. Currently, ESO is developing a high-speed 512x512 pixel eAPD array for AO applications with 64 parallel outputs which also may be used as a test device to demonstrate superior pixel performance for long integration times. Currently, diode structures are in development with an improved interdiffused multilayer process to mitigate the slight bandgap modulation causing the slow speed response and the persistence at low temperatures of T=40K [5][7]. Successful testing of radiation hardness and compatibility with operating the SAPHIRA array with the SIDECAR ASIC apart from the voltage for high APD gain show, that near infrared eAPD technology may soon be used also for space-based applications.

REFERENCES

[1] Finger, G., Smith, R., Menardi, S., Dorn, R., Meyer, M., Mehrgan, L., Stegmeier, J., Moorwood, A., "Performance limitations of small-format high-speed infrared arrays for active control loops in interferometry and adaptive optics", Optical and Infrared Detectors for Astronomy, Proc. SPIE 5499, (2004).

[2] Mehrgan, L., Eschbaumer, S., Finger, G., Meyer, M., Stegmeier, J.: "Performance and evaluation of the infrared AO sensor CALICO", Proc. SPIE 7021, High Energy, Optical, and Infrared Detectors for Astronomy III, (2008).

[3] Finger, G., Mehrgan, L., Ives, D., Eschbaumer, S., Baker, I., Dorn, R., Stegmeier, J., Meyer, M.," Development of high-speed, low-noise NIR HgCdTe avalanche photodiode arrays for adaptive optics and interferometry", Proc. SPIE. 7742, High Energy, Optical, and Infrared Detectors for Astronomy IV, (2010).

[4] Finger G., Baker I., Alvarez D., Ives D., Mehrgan L., Meyer M., Stegmeier J., Thorne P., Weller H, " Evaluation and optimization of NIR HgCdTe avalanche photodiode arrays for adaptive optics and interferometry ", Proc SPIE, Vol. 8453. 84530T, (2012).

[5] Finger G.; Baker I., Alvarez D., Ives D., Mehrgan L., Meyer M., Stegmeier J., Weller H.J., "SAPHIRA detector for infrared wavefront sensing", Proc. SPIE. 9148, Adaptive Optics Systems IV, 914817 (2014)

[6] Finger, G., Baker, I., Alvarez, D., Mehrgan, L., Stegmeier, J., Dupuy, C., Meyer, M., Weller, H., Ives, D.: "Sub-electron read noise and millisecond full-frame readout with the near infrared eAPD array SAPHIRA", Proc. SPIE. 9909, Adaptive Optics Systems V, (2016).

[7] Finger G., Ian Baker, I., Alvarez, D., Amorim, A., Brandner, W., Dupuy, C., Deen, C., Eisenhauer, F., Ives, D., Mehrgan, L., Meyer, M., Perraut, K., Perrin, G., Stegmeier, J., Straubmeier , C., Weller, H. C., "On-sky performance verification of near infrared e-APD technology for wavefront sensing and demonstration of e-APD pixel performance to improve the sensitivity of large science focal planes", Scientific Detector Workshop 2017 Proceedings, Baltimore, https://zenodo.org/communities/sdw2017/ (2017).

[8] Eisenhauer, F., Abuter, R. et al, Gravity Collaboration, "First light for GRAVITY: "Phase referencing optical interferometry for the Very Large Telescope Interferometer", Astronomy & Astrophysics, Volume 602, (2017).

[9] Eisenhauer F. et al, Gravity Collaboration, "Detection of the gravitational redshift in the orbit of the star S2 near the Galactic centre massive black hole", Astronomy & Astrophysics, Volume 615, (2018).

[10] Loose, M., Beletic, J., Blackwell, J., Garnett, J., Wong, S.," The SIDECAR ASIC — Focal Plane Electronics on a Single Chip", Cryogenic Optical Systems and Instruments XI, Proc. SPIE 5904, (2005).

[11] Finger, G., movie of test pattern: http://www.eso.org/~gfinger/heterojunction/chop_Hband_1ms.wmv

[12] Finger G., Baker I., Downing M., Alvarez D., Ives D.; Mehrgan L., Meyer M., Stegmeier J., Weller H. J., "Development of HgCdTe large format MBE arrays and noise-free high speed MOVPE eAPD arrays for ground based NIR astronomy", Proc. SPIE 10563, International Conference on Space Optics — ICSO 2014; 1056311 (2017).

[13] Baker, I., Maxey, C., Hipwood, L., Barnes, K.: "Leonardo (formerly Selex ES) infrared sensors for astronomy: present and future, Proc. SPIE 9915, High Energy, Optical, and Infrared Detectors for Astronomy VII, (2016).

[14] Hall, D., Baker, I., Goebel, S., Jacobson, S. Lockhart, C., Warmbier, E., Atkinson, D.: "Next-generation performance of SAPHIRA HgCdTe APDs", Proc. SPIE. 9915, High Energy, Optical, and Infrared Detectors for Astronomy VII, (2016).

[15] Atkinson, D., Hall, D., Jakobson, S., Baker, I.: "Dark Current in the SAPHIRA Series of APD Arrays", The Astronomical Journal, Volume 154, Issue6 (2017).
[16] Deen, C., Kolb, J., Oberti, H., Bonnet, E., Mueller, E. et al: System tests and on-sky commissioning of the GRAVITY-CIAO wavefront sensors, Proc. SPIE 9909, Adaptive Optics Systems V, 99092M (2016).
[17] Schmid, C., Abuter, R., Merand, A., Sahlmann, J., Alonso, et al.: Status of PRIMA for the VLTI: heading to astrometry, Optical and Infrared Interferometry III, Proc. SPIE 8445, (2012).
[18] Dorn, R. J., Eschbaumer, S., Finger, G., Ives, D., Meyer, M., Stegmeier, J., European Southern Observatory (ESO); "Sidecar Asic at ESO", Proc. SPIE 7742, (2010).
[19] Loose, M., "Application of the SIDECAR ASIC as the Detector Controller for ACS and the JWST Near-IR Instruments", Space Telescope Science Institute Calibration Workshop, (2010).
[20] Loose, M., Beletic, J., Blackwell, J., Garnett, J., , Wong, S., Hall, D., Jacobson, S., Rieke, M., Winters, G., "The SIDECAR ASIC — Focal Plane Electronics on a Single Chip", Proc.SPIE 5904, (2005).
[21] Goebel, S., Hall, D., Guyon, O., Warmbier, E., Jacobson, S., "Overview of the SAPHIRA Detector for AO Applications", Journal of Astronomical Telescopes, Instruments, and Systems (JATIS), to be published, (2018)
[22] Hall, D., Baker, I., Finger, G.: Towards the next generation of L-APD MOVPE HgCdTe arrays beyond the SAPHIRA 320 x 256, Proc. SPIE 9915, (2016).